

DATA ASSIMILATION ON A FLOOD WAVE PROPAGATION MODEL : EMULATION OF A KALMAN FILTER ALGORITHM

Assimilation de données sur un modèle d'onde de crue : émulation d'un algorithme de filtre de Kalman

Sébastien Barthélémy¹, Sophie Ricci
URA 1875/CERFACS, Toulouse, France
barthelemy@cerfacs.fr, ricci@cerfacs.fr

Olivier Pannekoucke
CNRM-GAME (Météo-France and CNRS) URA 1357, Toulouse, France
olivier.pannekoucke@meteo.fr

Olivier Thual
URA1875/CERFACS and INPT, CNRS, IMFT, Toulouse, France
thual@imft.fr

Pierre-Olivier Malaterre
UMR G-EAU, Irstea, Montpellier, France
p-o.malaterre@irstea.fr

KEY WORDS

Data assimilation ; real-time forecasting ; flood wave propagation model ; ensemble Kalman filter

ABSTRACT

This study describes the assimilation of synthetically-generated river water level observations in a flood wave propagation model. For this approach to be applied in the framework of real-time flood forecasting, the cost of the data assimilation procedure, mostly related to the estimation of the background error covariance matrix, should be bound. An Ensemble Kalman Filter (EnKF) algorithm is applied, with a steady observation network, to demonstrate how the assimilation modifies the background correlation function at the observation point. It is shown that an initially Gaussian correlation function turns into an anisotropic function at the observation point, with a shorter correlation length-scale downstream of the observation point than upstream, and that the variance of the error in the water level state is significantly reduced downstream of the observation point. The covariance matrix resulting from the EnKF is then used as an invariant background error covariance matrix for a series of successive Best Linear Unbiased Estimation (BLUE) algorithms which emulate an EnKF at a lower cost. This study shows how the background error covariance matrix can be computed off-line, with an advanced algorithm, and then used with a cheaper algorithm for real-time application.

1. INTRODUCTION

Flood forecasting is a key issue in hydrology and remains a challenging problem in operational hydrology. It has already been demonstrated that the limitations of the hydraulic models can be overcome using a data assimilation (DA) approach (Durand et al. [1], Ricci et al. [2], Jean-Baptiste et al. [3]). For most DA algorithms, the description of the background error covariance matrix is essential but generally fastidious and costly, which is not compatible with real-time forecasting. The aim of this study is to demonstrate how the cost of an Ensemble Kalman Filter (EnKF) algorithm can be reduced allowing for the use of DA in the framework of real-time flood forecasting. The model used for this study is a simplified and parsimonious hydraulic model, representing the 1D diffusive flood wave propagation equations.

¹ Corresponding author

A key point of the paper relies on the evolution of correlation functions of the water level state by both the intrinsic dynamics of the model and the data assimilation process. When imposing an upstream flow forcing as a random signal of gaussian statistics with a gaussian shaped temporal covariance function, the water level states are random functions whose spatial covariance functions can be approximated, when the diffusion is small compared to the advection, by a Gaussian with an increasing correlation length-scale. This results can be shown analytically and is illustrated here by a numerical ensemble approach.

However, when the water level profiles are corrected through a data assimilation procedure, the theoretical description of the evolution of the correlation function is not straightforward and a numerical approach is preferred. An EnKF algorithm was thus applied, with a steady observation network (in terms of location, frequency and error statistics), to demonstrate how the assimilation modifies the background correlation function at the observation points. It was shown that an initial correlation function of Gaussian shape turns into an anisotropic² function at the observation point, with a shorter correlation length-scale downstream of the observation point than upstream, and that the error variance of the state is significantly reduced downstream of the observation point. The use of the information brought by the observations as well as by the implicit propagation of the background error covariance function by the EnKF algorithm, leads to the formulation of a steady covariance matrix, different from the Gaussian initially prescribed in the system. This matrix was finally used as an invariant background error covariance matrix for an ensemble of assimilation runs to emulate an EnKF. This paper presents how the results from this Emulated EnKF algorithm (EEnKF) and from the EnKF algorithm compare. Additionally, the reduction of the error variance and the correlation length downstream of the observation point was formulated as a function of the ratio between the background and the observation error standard deviation at the observation point. Using this information, the EnKF can be emulated for observation networks that differ in terms of error statistics.

The outline of the paper is as follows: Section 2 describes the diffusive flood wave propagation model. It also provides theoretical proof for the generation of a signal with a Gaussian spatial covariance function and for the evolution of the correlation function and length-scale without assimilation. The numerical validation, with an ensemble approach, for these theoretical results is presented as well. A brief description of the ensemble based DA algorithms used in the paper is then given in Section 3. The results of the EnKF and EEnKF algorithms regarding the evolution of water level and its error statistics are finally outlined. Some conclusive remarks and perspectives are given in Section 4.

2. THE DYNAMICS OF THE FLOOD WAVE PROPAGATION MODEL

2.1 Model equations and boundary conditions

In the framework of the diffusive flood wave approximation, the Saint Venant equations can be crudely approximated as

$$\frac{\partial h}{\partial t} + c \frac{\partial h}{\partial x} = \kappa \frac{\partial^2 h}{\partial x^2}, \quad (1)$$

where the water level is described as a perturbation h to the equilibrium state (h_n, U_n) such that $U_n = K_s (\sin \gamma)^{\frac{1}{2}} h_n^{\frac{2}{3}}$ (with K_s the Strickler coefficient), $\kappa = \frac{U_n h_n}{2 \tan \gamma}$ for a constant slope γ on a 1D domain defined for $x \in [0, L]$, with $L = 200$ km and discretised in 200 points. Eq. (1) is a classical advection-diffusion equation where κ is the diffusion coefficient, $c = \frac{5U_n}{3}$ is the advection speed and h is the Water Level Anomaly (WLA). In order to use this model as a support for data assimilation, an open boundary condition is imposed downstream with $\frac{\partial h}{\partial t}(L, t) + c \frac{\partial h}{\partial x}(L, t) = 0$. The upstream boundary condition is imposed by $h(0, t) = q(t)$, where q is characteristic of a flow up to a multiplicative constant. Here, q is modelled as a stationary Gaussian random process characterised by a temporal covariance function in time $\rho(\delta t) =$

$\langle q(t)q^*(t + \delta t) \rangle$ that has gaussian shape of correlation time scale τ , $\rho(\delta t) = q_m^2 e^{-\frac{\delta t^2}{2\tau^2}}$. Using Fourier transform, $q(t)$ can be written as a sum of harmonic signals³ $q(t) = \int_{\mathbb{R}} q_\omega e^{-i\omega t} d\omega$. Due to the stationarity

² The function is not symmetric with respect to the observation point

³ We use this sign convention to obtain a propagative solution along increasing x for positive t .

of the random process, the complex amplitudes q_ω are uncorrelated so that $\langle q_\omega q_{\omega'}^* \rangle = \rho_\omega \delta(\omega - \omega')$, where δ is the Dirac distribution and where the energy spectrum $\rho_\omega = \frac{\tau}{\sqrt{2\pi}} q_m^2 e^{-\frac{\omega^2 \tau^2}{2}}$ is the Fourier transform of $\rho(\delta t) = \int_{\mathbb{R}} \rho_\omega e^{-i\omega \delta t} d\omega$ (Wiener-Khintchine theorem). From a numerical point of view, the amplitudes q_ω can be built as $q_\omega = \sqrt{\rho_\omega} \zeta_\omega$ where ζ_ω is a complex Gaussian random variable whose module has zero mean and standard deviation 1 and $\zeta_\omega = \zeta_{-\omega}^*$.

2.2 Covariance function for the WLA

Knowing the characteristics of the temporal covariance of the boundary condition flow $q(t)$, the spatial covariance of the WLA state can be derived. Given the linearity of the problem, the solution $h(x, t)$ can be formulated as the superposition of modal solutions. Assuming that the forcing is a sinusoidal function $q(t) = q_\omega e^{-i\omega t}$, a modal solution for Eq. 1 reads $h(x, t) = q_\omega e^{-i\omega t} h_\omega(x)$ and the general solution reads $h(x, t) = \int_{\mathbb{R}} q_\omega e^{-i\omega t} h_\omega(x) d\omega$.

In the case of advection only ($\kappa = 0$), $h_\omega(x) = e^{i\omega \frac{x}{c}}$ of which the covariance function Σ is a gaussian of constant length-scale $L_0 = c\tau$, defined as :

$$\Sigma(x, x + \delta x) = \langle h(x, t) h^*(x + \delta x, t) \rangle = \int_{\mathbb{R}} \rho_\omega e^{-i\omega \frac{\delta x}{c}} d\omega = \rho\left(\frac{\delta x}{c}\right), \quad (2)$$

In the case of advection with small diffusion, which reads $\kappa \ll cx$, a straightforward expansion leads to $h_\omega(x) = e^{\left(\frac{c}{2\kappa} - \frac{\sqrt{c^2 - 4i\omega\kappa}}{2\kappa}\right)x} \simeq e^{i\omega \frac{x}{c} - \frac{\omega^2 \kappa}{c^3} x}$, and a more elaborated asymptotic analysis shows that Σ can locally be approximated by

$$\Sigma(x, x + \delta x) \simeq \int_{\mathbb{R}} \frac{q_m^2}{\sqrt{2\pi}} L_p(0) e^{-\frac{\omega^2 L_p^2(x)}{2}} e^{-i\omega \delta x} d\omega = q_m^2 \frac{L_p(0)}{L_p(x)} e^{-\frac{\delta x^2}{2L_p^2(x)}}, \quad (3)$$

that is a Gaussian covariance function of correlation length-scale :

$$L_p(x) = \sqrt{L_p^2(0) + 4\kappa \frac{x}{c}}, \quad (4)$$

and variance :

$$q_m^2 \frac{L_p(0)}{L_p(x)}. \quad (5)$$

2.3 Validation with an ensemble approach

These theoretical results were validated computing the covariance matrix \mathbf{B}_e of an ensemble of $[N_e]$ WLA states $\mathbf{x}^k = (h_{1,k}, \dots, h_{N_e,k})$ on the 1D domain $[0, L]$, generated with different forcings $q_k(t)$ with $k \in [1, N_e]$ that follows the statistics described in Sect. 2.1. The correlation length-scale L_p is computed with the correlation function ρ between two points distant of δx and $L_p = \frac{\delta x}{2\sqrt{1-\rho(\delta x)}}$ (Pannekoucke and al. [4]).

Figure 1-a displays the covariance δx -functions $\Sigma(x, x + \delta x)$ at three different points x of the 1D domain for the advection only case (dashed lines) and for the advection-diffusion case (solid lines), for $N_e = 10000$. In the first case, the initially Gaussian function is advected. The characteristics of the covariance function remain unchanged as illustrated in Fig. 1-b where L_p is constant (dashed thick line), in agreement with the theoretical value (dashed thin line). When diffusion occurs, the covariance function of the WLA state is diffused as shown in Fig. 1-a and $L_p(x)$ increases with x (solid thick line on Fig 1-b), still in agreement with the theoretical value (solid thin line). The WLA variance initially prescribed at 1 m² remains constant for the advective case and decreases with x for the diffusive case as described in Fig.1-a (amplitude max of the covariance functions in solid line).

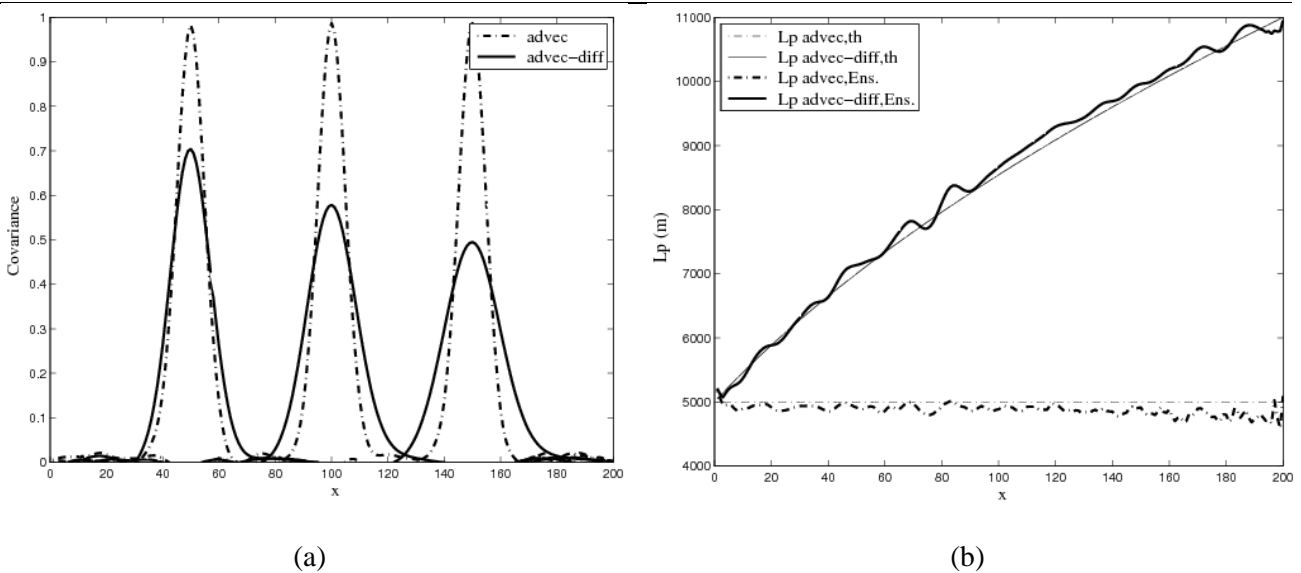


Figure 1: (a) Covariance δx -function $\Sigma(x, x + \delta x)$ from \mathbf{B}_e for $x = 50, 100, 150$, (b) Correlation length-scale $L_p(x)$

3. THE DYNAMICS OF THE FLOOD WAVE PROPAGATION MODEL

3.1 Data assimilation algorithms

The EnKF algorithm was implemented on Eq. (1), using the identical-twin experiment framework (also known as OSE⁴). A reference run was integrated using a given forcing $q^{true}(t)$, to simulate the *true* WLA h^{true} . The observation $h^{obs}(t) = h^{true}(t) + \epsilon^o(t)$ was then calculated in the middle of the 1D domain ($x_{obs} = \frac{L}{2}$) where $\epsilon^o(t)$ is a Gaussian noise defined by its standard deviation σ^o , thus defining the observation vector⁵ \mathbf{y}^o . The background trajectories $h_k^b(x, t)$ for the ensemble approach were integrated using a perturbed set of forcing $q_k(t)$ with $k \in [1, N_e]$, defining the background vectors $\mathbf{x}^{b,k}$. The observation frequency is equal to 3 model time steps.

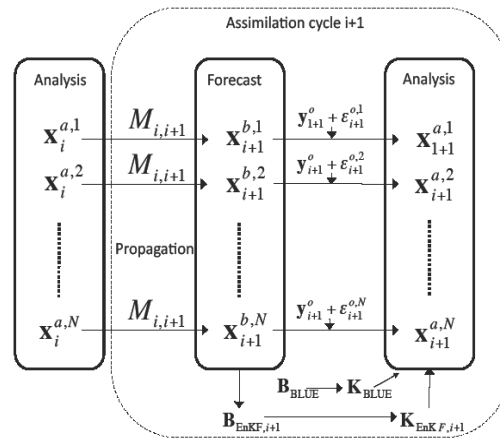


Figure 2: Ensemble data assimilation algorithms, assimilation cycle $i + 1$.

As illustrated on Fig. 2 for the assimilation cycle $i + 1$, the ensemble analysed states $\mathbf{x}_i^{a,k}$ are propagated by the diffusive flood wave model $M_{i,i+1}$ from the observation time i to $i + 1$ to provide the background states $\mathbf{x}_{i+1}^{b,k} = M_{i,i+1}(\mathbf{x}_i^{a,k})$ over which the background error covariance matrix $\mathbf{B}_{EnKF,i+1}$ is computed. The

⁴ Observing System Experiment

⁵ here \mathbf{y}^o is a scalar

assimilation step at $i + 1$ consists in assimilating a perturbed observation vector $\mathbf{y}_{i+1}^o + \epsilon_{i+1}^{o,k}$ to correct the background vector $\mathbf{x}_{i+1}^{b,k}$, using the Kalman filter gain matrix $\mathbf{K}_{\text{EnKF},i+1}$:

$$\mathbf{x}_{i+1}^{a,k} = \mathbf{x}_{i+1}^{b,k} + \mathbf{K}_{\text{EnKF},i+1} \left(\mathbf{y}_{i+1}^o + \epsilon_{i+1}^{o,k} - \mathbf{H}(\mathbf{x}_{i+1}^{b,k}) \right) \quad (6)$$

$$\mathbf{K}_{\text{EnKF},i+1} = \mathbf{B}_{\text{EnKF},i+1} \mathbf{H}^T (\mathbf{H} \mathbf{B}_{\text{EnKF},i+1} \mathbf{H}^T + \mathbf{R})^{-1}, \quad (7)$$

After 1000 assimilation cycles, $\mathbf{B}_{\text{EnKF},i}$ converges to a steady matrix denoted \mathbf{B}_{EnKF} (its associated correlation matrix is \mathbf{C}_{EnKF}). The BLUE⁶ algorithm can be viewed as a Kalman Filter in which the ensemble is replaced by one single forcing $q(t)$ with the gain matrix :

$$\mathbf{K}_{\text{BLUE}} = \mathbf{B}_{\text{BLUE}} \mathbf{H}^T (\mathbf{H} \mathbf{B}_{\text{BLUE}} \mathbf{H}^T + \mathbf{R})^{-1}, \quad (8)$$

where \mathbf{B}_{BLUE} is a constant matrix. This DA method can of course be applied to an ensemble of forcings $q_k(t)$ at successive time t_i and a comparison of the results of the EnKF and this ensemble of BLUE algorithms can be made, as pictured in Fig. 2.

With the choice $\mathbf{B}_{\text{BLUE}} = \mathbf{B}_e$, one misses the fact that the background error covariance matrix should be impacted by the previous assimilation steps. In the following, the ensemble of BLUE analysis using $\mathbf{B}_{\text{BLUE}} = \mathbf{B}_e$ is called the EnBLUE algorithm and the covariance matrix computed over the assimilated members is denoted by $\mathbf{B}_{\text{EnBLUE}}$. If one chooses $\mathbf{B}_{\text{BLUE}} = \mathbf{B}_{\text{EnKF}}$ where \mathbf{B}_{EnKF} is the converged matrix previously computed, the reduction of uncertainty brought by the previous BLUE steps is likely to be represented, at least after several time steps. This ensemble based approach emulates the EnKF algorithm but saves the computational cost of the time evolving background error matrix. It is named here Emulated Kalman Filter (EEnKF). In the following, the ensemble of BLUE analysis using $\mathbf{B}_{\text{BLUE}} = \mathbf{B}_{\text{EnKF}}$ is called the EEnKF algorithm and the covariance matrix computed over the assimilated members is denoted by $\mathbf{B}_{\text{EEnKF}}$.

3.2 Data Assimilation results

The initial background covariance matrix prescribed for the assimilation system is \mathbf{B}_e , its associated correlation function is noted \mathbf{C}_e . Figure 3-a illustrates how the initially isotropic correlation function in \mathbf{C}_e (dashed line) is modified by the analysis and propagation steps of the EnKF algorithm, at the end of the assimilation procedure. Considering a steady observation network, the shape of the correlation function in \mathbf{C}_{EnKF} (solid line) converges towards an anisotropic correlation function with a shorter correlation length-scale downstream of the observation point than upstream. The correlation between the observation point and its neighbours is reduced since information at the observation point was introduced at this location by the analysis procedure through the observation vector.

The correlation length-scale L_p is computed for both EnBLUE and EnKF algorithms. As presented on Fig. 3-b, the evolution of the correlation length-scale on the 1D domain follows the theory (solid thin line) upstream of the observation point and a discontinuity is introduced at the observation point. For the EnKF algorithm (solid thick line), the reduction of the correlation length-scale spreads over the entire domain downstream of the observation point, where as for the EnBLUE algorithm (dashed thin line), this reduction is local.

⁶ Best Linear Unbiased Estimator

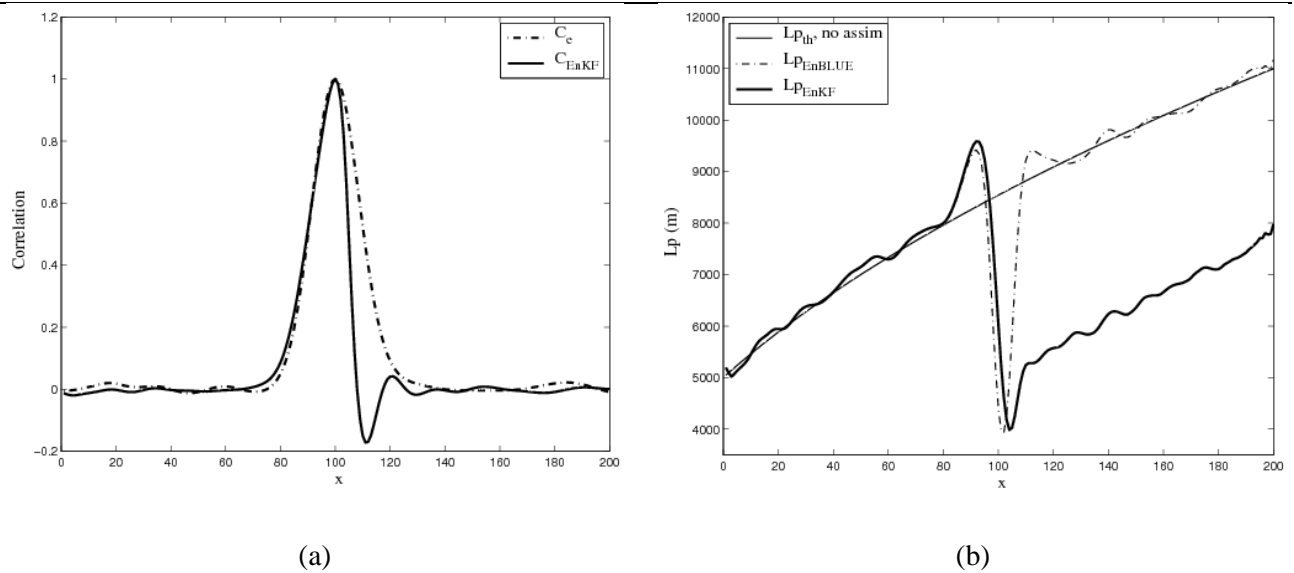


Figure 3 : (a) Correlation function at the observation point, for the initial correlation matrix C_e (dashed line) and for C_{EnKF} (solid line). (b) Correlation length-scale $L_p(x)$ in theory without assimilation (thin solid line), for B_{EnBLUE} (thin dashed line) and B_{EnKF} (thick solid line).

In order to estimate the impact of the EnBLUE, EnKF and EEnKF algorithms, the variances of the background error covariance matrix are presented in Fig. 4-a. The error variance is significantly reduced at the observation point and beyond with the EnKF (solid thick line), compared to the initially prescribed variances (solid thin line). However, when B is kept invariant and isotropic, the reduction of the variance is only located in the close neighboring of the observation point (dashed thin line); the invariant matrix is not optimal and the EnBLUE algorithm overcorrects the state downstream of the observation point. In this case, the merits of using a DA algorithm that evolves the background error statistics with the dynamics are demonstrated; the shorten length-scale of B_{EnKF} prevents from overcorrecting downstream of the observation once information from the observation was taken into account. The EEnKF algorithm shows the same results as the EnKF meaning that the computation of the EnKF evolved background covariance matrix can be achieved at first and then used for further assimilation with a reduced computational cost.

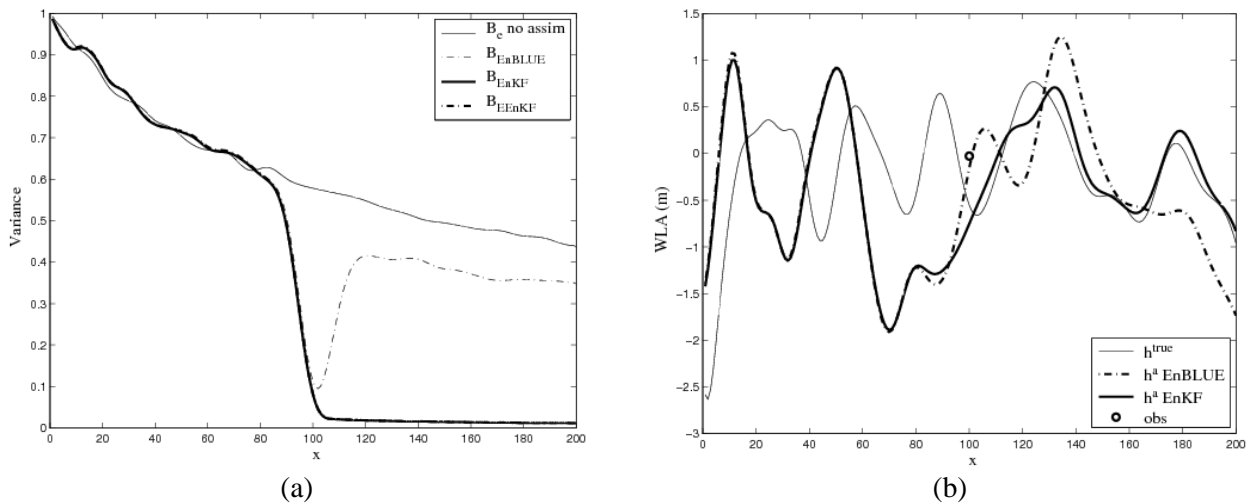


Figure 4 : (a) Background error variances for the initial covariance matrix B_e without assimilation (thin solid line), for B_{EnBLUE} (thin dashed line), for B_{EnKF} (thick solid line) and for B_{EEnKF} (thick dashed line) (b) WLA for the BLUE analysis with B_e (thick dashed line for h^a_{EnBLUE}) and B_{EnKF} (thick solid line for h^a_{EnKF}). The observation is denoted by a circle, the true state h^{true} by a thin solid line.

This result is of particular interest in the framework of real-time forecasting where a single analysis is usually carried out instead of an ensemble of analysis (what we are looking for is the forecasted WLA state and not its covariance matrix). Assuming that an EnKF analysis has previously been carried out, the real-

time data assimilation procedure can be achieved with a non expensive BLUE algorithm, using \mathbf{B}_{EnKF} as the invariant background error covariance matrix for a single analysis. This idea was implemented here, the improvement of the WLA for a BLUE analysis using \mathbf{B}_e or $\mathbf{B}_{\text{EEnKF}}$ is shown in Fig. 4-b. When the BLUE assimilation is carried with $\mathbf{B}_{\text{BLUE}} = \mathbf{B}_{\text{EnKF}}$ the analysed state h^a EEnKF (thick solid line) is significantly close to the *true* state h^{true} (thin solid line) at the observation point and beyond. On the contrary when the assimilation is carried with $\mathbf{B}_{\text{BLUE}} = \mathbf{B}_e$, the analysed state h^a EnBLUE (thick dashed line) is only locally brought closer to the true state at the observation point.

3.3 Extension of the results to an observation network with different error statistics

Section 3.2 showed that the asymptotic background error covariance matrix of the EnKF can be used as an invariant matrix within a non expensive BLUE algorithm to emulate the EnKF. At the observation point, the reduction on the error variance and the downstream correlation length scale are well reproduced. Both depend on the ratio $r = \frac{\sigma_{b,\text{ini}}}{\sigma_o}$ (where $\sigma_{b,\text{ini}}$ and σ_o respectively denote the background without assimilation and observation error standard deviations at the observation point) and should be evaluated as r varies ($\sigma_{b,\text{ini}}$ is assumed to be fixed and σ_o varies to represent different observation error statistics).

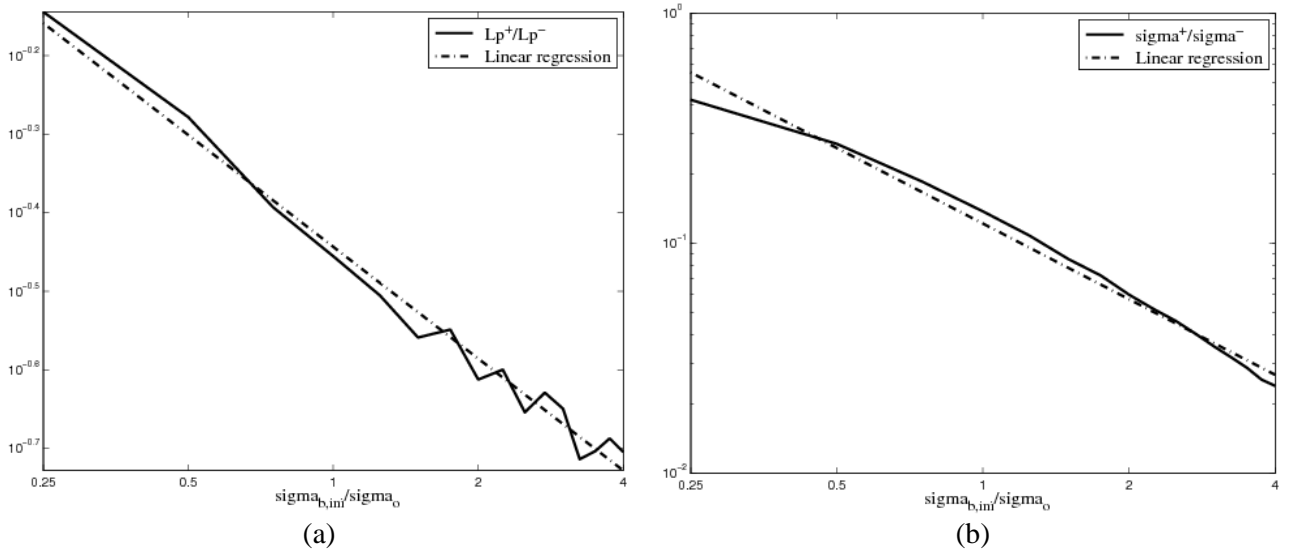


Figure 5 : Abacus for (a) $\frac{L_p^+}{L_p^-}$ and (b) $\frac{\sigma^+}{\sigma^-}$ as function of the ratio $r = \frac{\sigma_{b,\text{ini}}}{\sigma_o}$.

In order to quantify the anisotropy $\frac{L_p^+}{L_p^-}$ at the observation point, a set of EnKF experiments were carried out for $r \in [0.25; 4]$ and leads to the construction of an abacus Fig. 5-a. Similarly, an abacus was achieved to quantify the reduction of the variance error $\frac{\sigma^+}{\sigma^-}$ at the observation point (Fig. 5-b). Globally, the error variance reduction and the anisotropy decrease when the observation error increases. A linear regression in logarithmic scale leads to :

$$\begin{aligned} \ln\left(\frac{L_p^+}{L_p^-}\right) &= \alpha \ln\left(\frac{\sigma_{b,\text{ini}}}{\sigma_o}\right) + \beta \\ \ln\left(\frac{\sigma_b^2}{\sigma_{b,\text{ini}}^2}\right) &= \gamma \ln\left(\frac{\sigma_{b,\text{ini}}}{\sigma_o}\right) + \delta \end{aligned} \quad (9)$$

Away from the observation point, $L_p(x)$ and $\sigma^2(x)$ are derived from the analytical expressions (4) and (5) :

$$\begin{aligned} L_p^2(x) &= L_p^2(0) + 4\kappa \frac{x}{c} & x < x_{\text{obs}} \\ L_p^2(x) &= (L_p^+)^2 + 4\kappa \frac{x-x_{\text{obs}}}{c} & x_{\text{obs}} < x \end{aligned} \quad (10)$$

$$\begin{aligned}\sigma^2(x) &= q_m^2 \frac{L_p(0)}{\sqrt{L_p^2(0) + 4\kappa \frac{x}{c}}} & x < x_{obs}, \\ \sigma^2(x) &= \sigma_b^2 \frac{L_p^+}{\sqrt{(L_p^+)^2 + 4\kappa \frac{x-x_{obs}}{c}}} & x_{obs} < x.\end{aligned}\tag{11}$$

Thus for any observation error variance σ_o , the impact of the assimilation can be estimated using Eqs. (9-11). The covariance function is fully described for all x by $L_p(x)$ and $\sigma(x)$ and the asymptotic background error covariance matrix \mathbf{B}_{EnKF} can be built without integrating the EnKF algorithm. Finally this matrix is to be used with the BLUE algorithm as described in Section 3.2 to emulate an EnKF with a reduced computational cost, consistently with the real-time analysis constraints for flood forecasting.

4. CONCLUSION

This study describes how the evolution of the background error covariance matrix with an EnKF algorithm provides the optimal matrix for the assimilation system with a diffusive flood wave propagation model and steady observation network. The resulting correlation function at the observation point is anisotropic as the assimilation and propagation steps tend to shorten the correlation length-scale downstream of the observation point. The anisotropy introduced at the assimilation cycle i has an impact on cycle $i + 1$ and the dynamics of the covariance matrix should be taken into account. The evolved covariance matrix from EnKF can be used as an invariant matrix. This approach leads to the same result as the EnKF but with a much reduced computational cost, allowing for the use of DA for real-time flood forecasting. Finally the anisotropy in the correlation length as well as the reduction of the error variance resulting from the EnKF assimilation were described by abacus, as linear functions of the observation error variance. Thereby, once the abacus are built, the background error covariance matrix is fully described and the emulation of the EnKF can be achieved for other observation networks with any observation error variance. The solution for building the background error covariance matrix using prescribed anisotropic correlation lengths and variances is not developed in this paper. The use of a diffusion equation to do so is described in Weaver and Mirouze [6] and will be applied to the present study in further work.

ACKNOWLEDGEMENTS

The authors would like to thank LNHE, the SCHAPI and Andrea Piacentini for their contribution.

REFERENCES AND CITATIONS

- [1] Durand M., Andrealis K., Alsdorf D., Lettenmaier D., Moller D., Wilson M. (2008). Estimation of bathymetric depth and slope from data assimilation of swath altimetry into a hydrodynamic model, *GRL*, Vol. 35, L20401.
- [2] Ricci S., Piacentini A., Thual O., Le Pape E., Jonville G. (2011). Correction of upstream flow and hydraulics state with data assimilation in the context of flood forecasting, *Hydrol. Earth Syst. Sci*, Vol. 15, 1-21.
- [3] Jean-Baptiste N., Malaterre P.-O., Dorée C., Sau J. (2011). Data assimilation for real-time estimation of hydraulic states and unmeasured perturbations in a 1D hydrodynamic model, *Journal of Mathematics and Computers in Simulation*, Vol. 81, Issue 10, pp 2201-2214.
- [4] Pannekoucke O., Berre L., Desroziers G. (2008). Background error correlation length-scale estimates and their sampling statistics. *Q. J. R. Meteorol. Soc.*, Vol. 134, 497-508.
- [5] Evensen G. (2009) *Data Assimilation - The Ensemble Kalman Filter*, Springer.
- [6] Weaver A., Mirouze I. (2012) : On the diffusion equation and its application to isotropic and anisotropic correlation modelling in variational assimilation. *Q. J. R. Meteorol. Soc.*, in press.